Giornata Seminariale Progetto RE-FRESCOS

Giovedì 1 Luglio, 2010, Aula Albenga (DISTR)

Emissioni acustiche ed elettromagnetiche durante la propagazione della frattura

A. Carpinteri, G. Lacidogna, A. Manuello

Department of Structural Engineering and Geotechnics, Politecnico di Torino, Italy

G. Niccolini, A. Schiavi, A. Agosto

National Research Institute of Metrology – INRiM, Italy

In this work we investigate the mechanical behaviour of concrete and rocks specimens loaded up to failure by the analysis of Acoustic Emission (AE) and Electromagnetic Emission (EME).

All specimens were tested in compression at a constant displacement rate and monitored by piezoelectric (PZT) transducers for AE data acquisition.

Simultaneous investigation of magnetic activity was performed by a measuring device calibrated according to metrological requirements.

In all the considered cases, the presence of AE events has been always observed during the damage process.

In the same tests EME signals were generally observed only in correspondence of the final collapse or sharp stress drops.

The Acoustic Emission Technique

Cracking is accompanied by the emission of elastic waves which propagate within the bulk of the material.

These waves can be received by transducers applied to the surface of the structura elements.

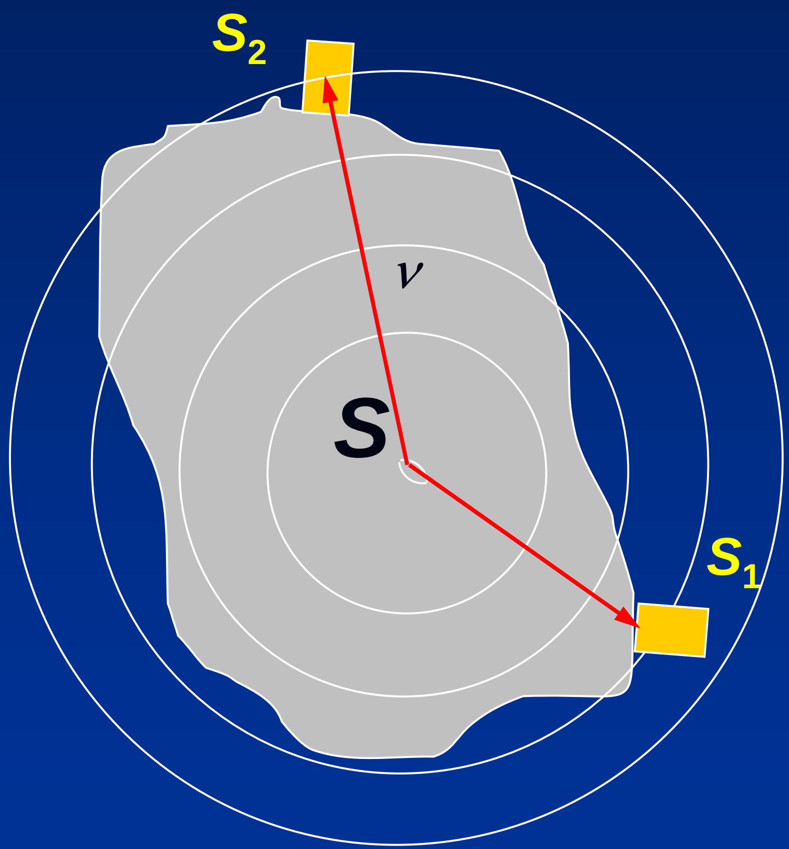

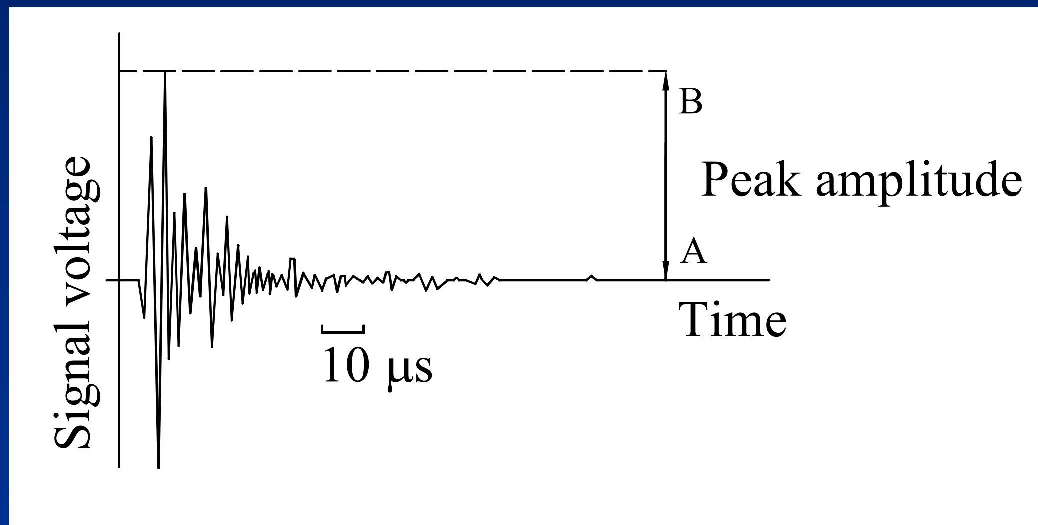

The adopted sensors are PZT transducers (50-500 kHz), and PZT accelerometric transducers (1-10kHz).

Typical AE signals detected during compression tests

AE-HF signals due to particle vibration around their equilibrium position.

AE-LF signals due to relevant oscillations of the entire specimen.

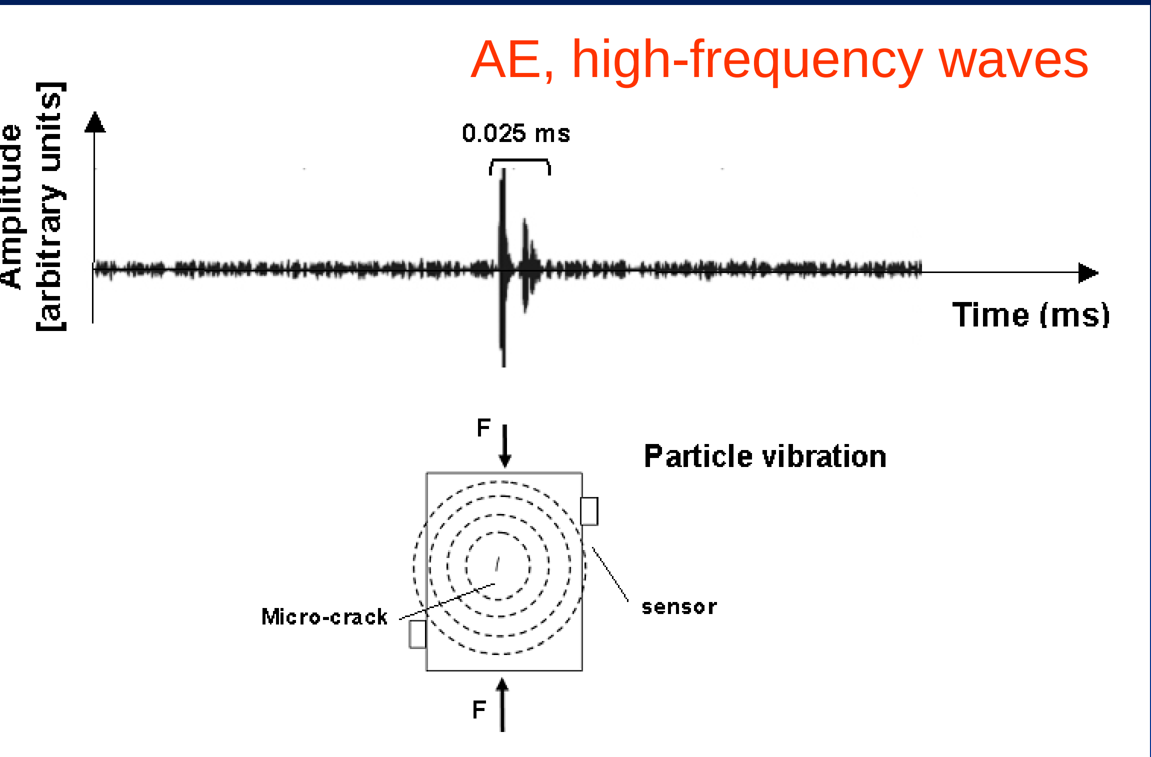

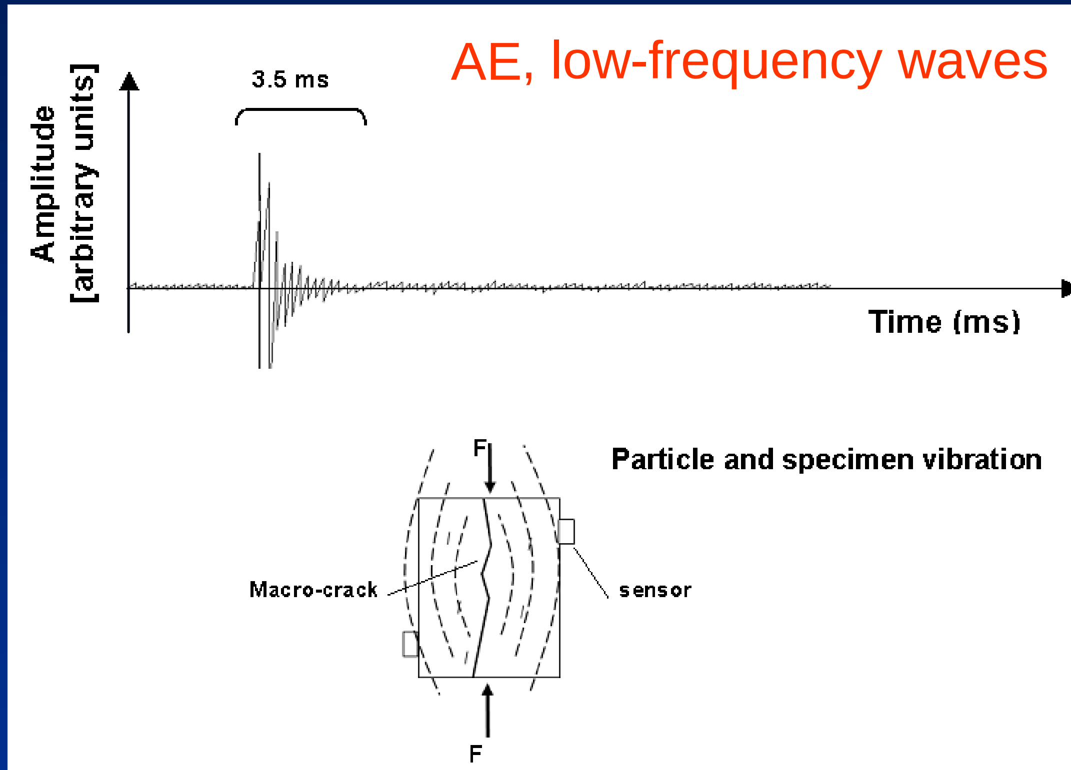

AE-HF signals:

- duration ~ 0.025 ms
- frequency ~ 200 kHz
- wavelength ~ 0.02 m

AE-LF signals:

- duration ~ 3.5 ms
- frequency ~ 6 kHz
- wavelength ~ 0.66 m

Typical EM signal detected during compression tests

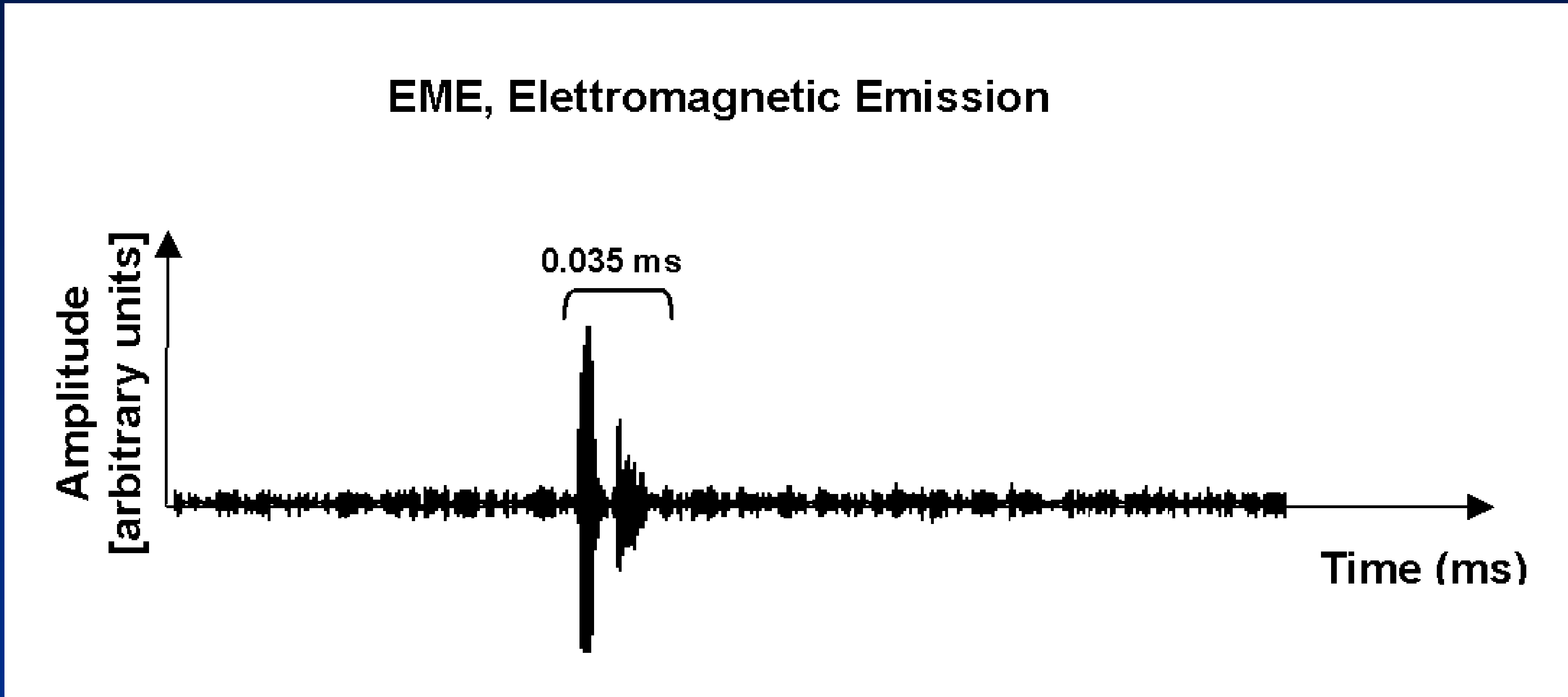

The analysed time duration of the EME is almost similar to the AE duration.

The main frequency is close to 160 kHz according to the working frequency range (10 Hz and 400 kHz) of the adopted device.

AE Data acquisition system

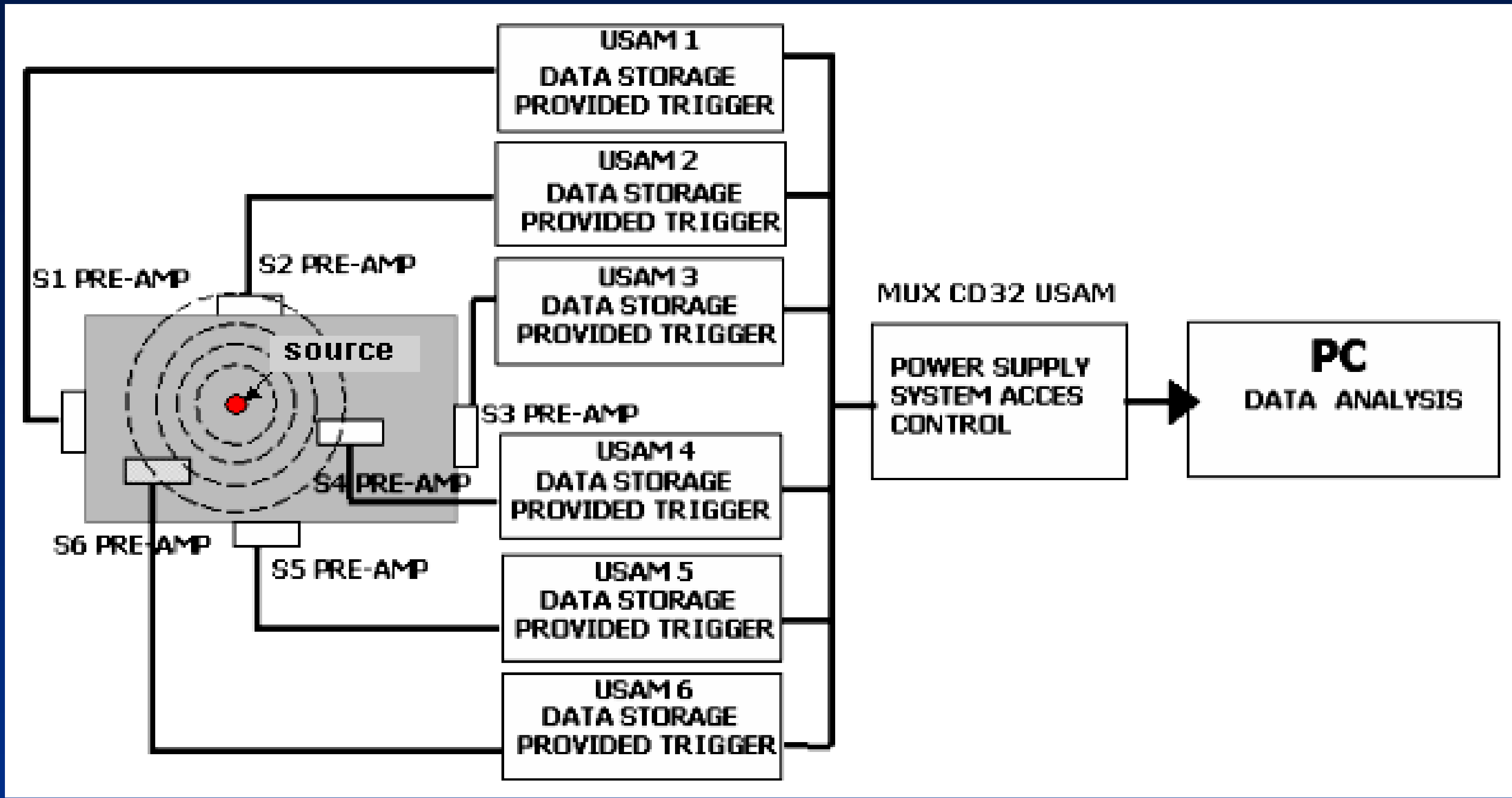

- **PZT transducers are set on a frequency range between 50 kHz and 500 kHz.**
- **Data acquisition system consisting in: 6 Pre-Amplified sensors, 6 Data storage provided trigger, a central unit for the synchronization phase, a threshold measurer.**
- **From this elaboration microcracks localisation is performed and the condition of the monitored specimen can be determined.**

AE counting method

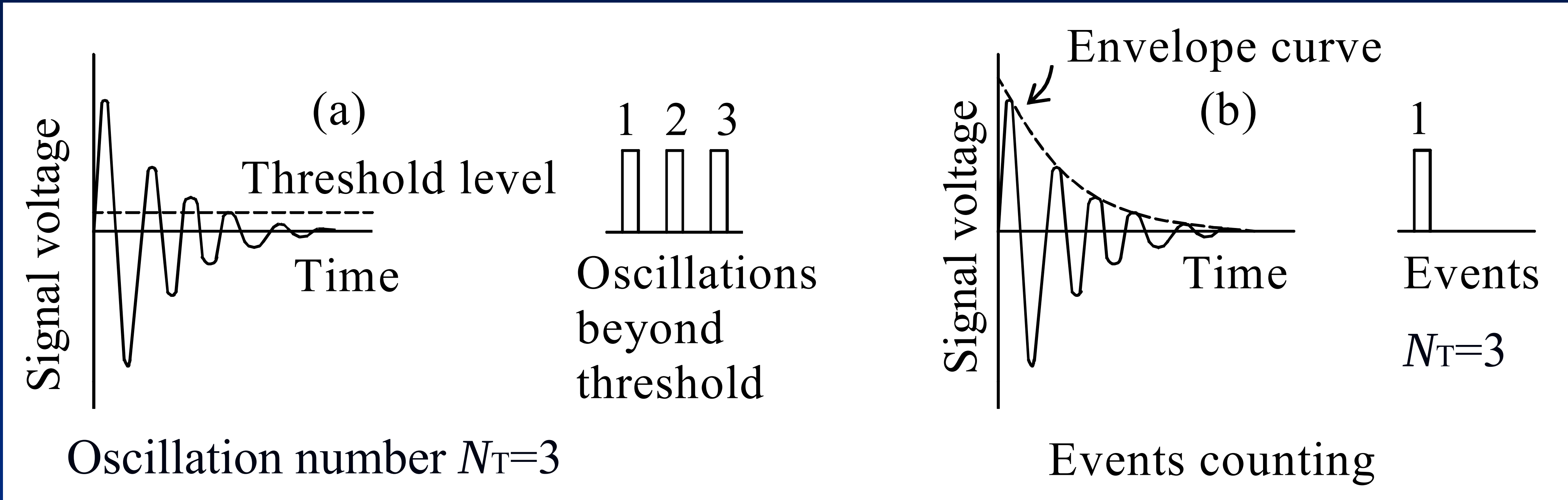

- **The event intensity is measured by the oscillation number N_T.**
- **The oscillation number N_T increases with the signal amplitude.**

As a first approximation, the number of counts *N* can be compared with the quantity of energy released during the loading process, and we may assume that the corresponding increments grow proportionally to the widening of the crack faces.

AE behaviour of a quasi-brittle material in compression

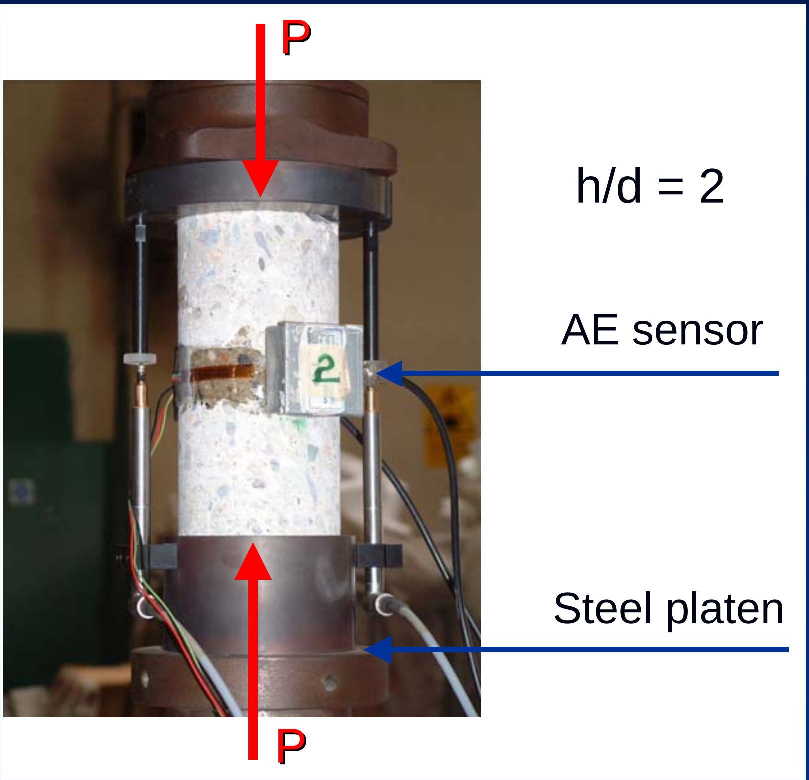

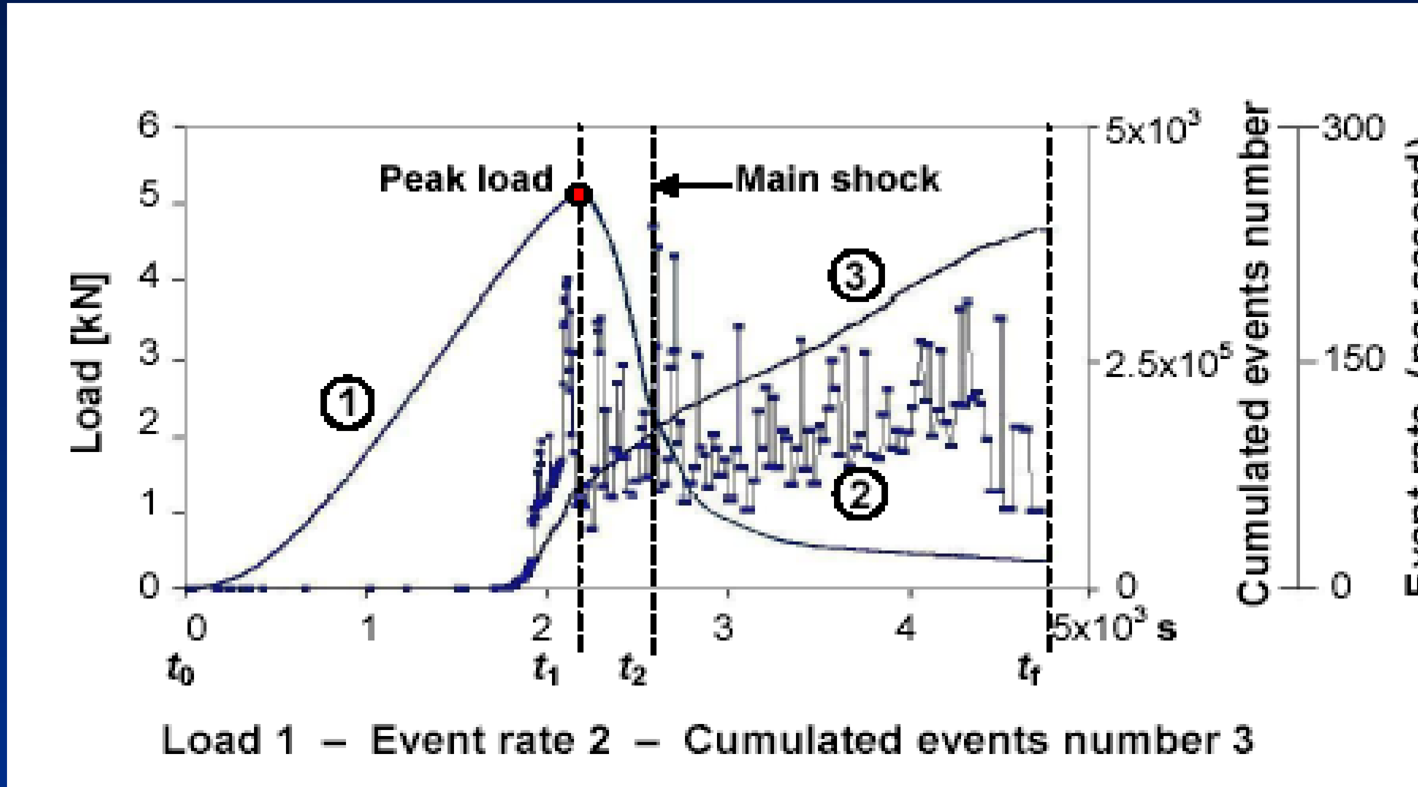

The compression test were performed in displacement control, by imposing a constant rate of displacement of the upper loading platen.

Compressive load vs. time, cumulated event number, and event rate (for each second of the testing period) are depicted in this figure.

AE signals amplitude distribution [I] [II]

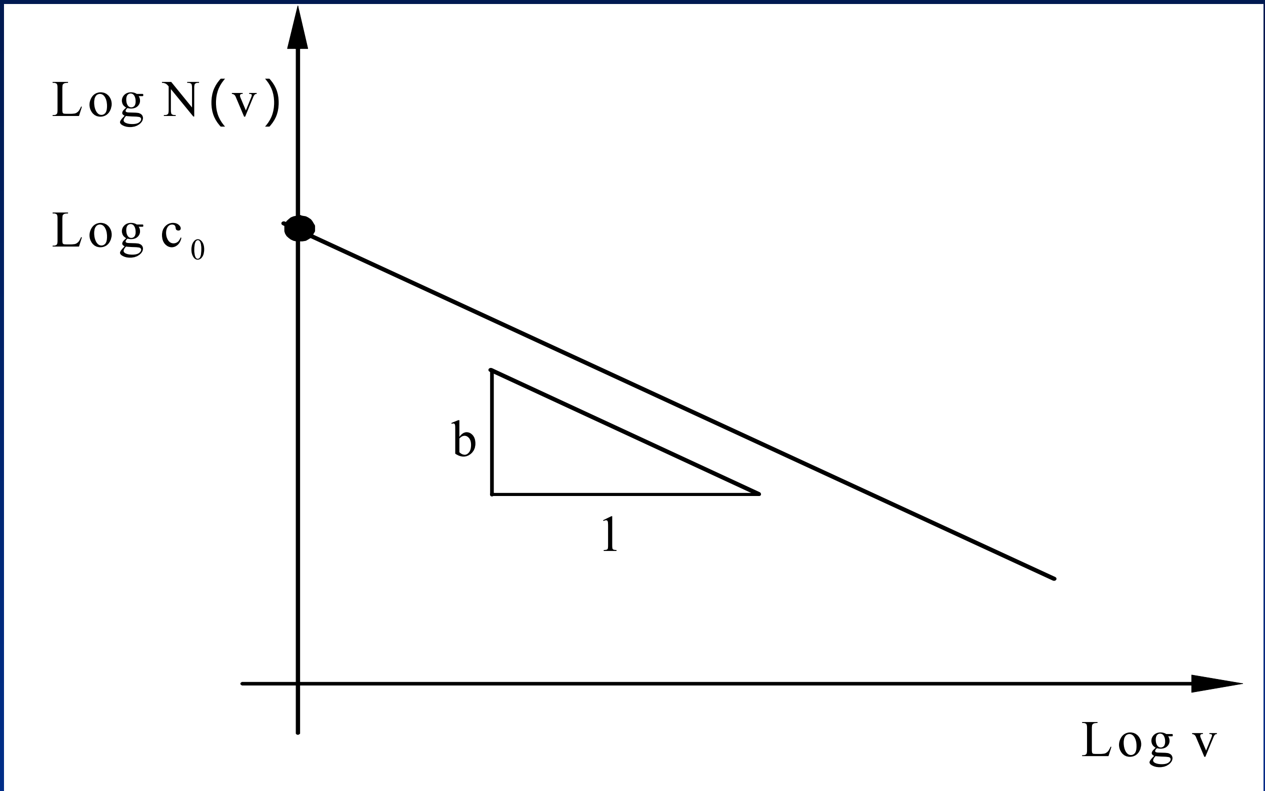

Cumulative signals distribution

$$N(v) = \int_{v}^{\infty} n(v_p)dv_p$$

$$N(v) = c_o v^{-b}$$

$$\mathrm{Log}\, N(v) = \mathrm{Log}\, c_o - b\,\mathrm{Log}\, v$$

Energy calculation

$$E(t) = \int_{v}^{\infty} v_P^2 n(v_p)dv_p \quad [J/s]$$

(I) Carpinteri, A., "Scaling laws and renormalization groups for strength and toughness of disordered materials". *Int. Journal of Solids and Structures*, 31, 291-302 (1994).

(II) Carpinteri, A., Lacidogna, G., Niccolini, G., "Fractal analysis of damage detected in concrete structural elements under loading", *Chaos, Solitons & Fractals*, 42, 2047-2056 (2009).

EM emission acquisition system

- The adopted device –Narda ELT 400 exposure level tester– works in the frequency range between 10 Hz and 400 kHz.
- The measurement range is between 1 nT to 80 mT.
- The tri-axial measurement system has a 100 cm^2 magnetic field sensor for each axis.
- This device was placed 1 m away from the specimens.

Data acquisition of the EME signals was triggered when the magnetic field exceeded the <u>threshold fixed at 0.2 µT</u> after preliminary measurements to filter out the magnetic noise in the laboratory.

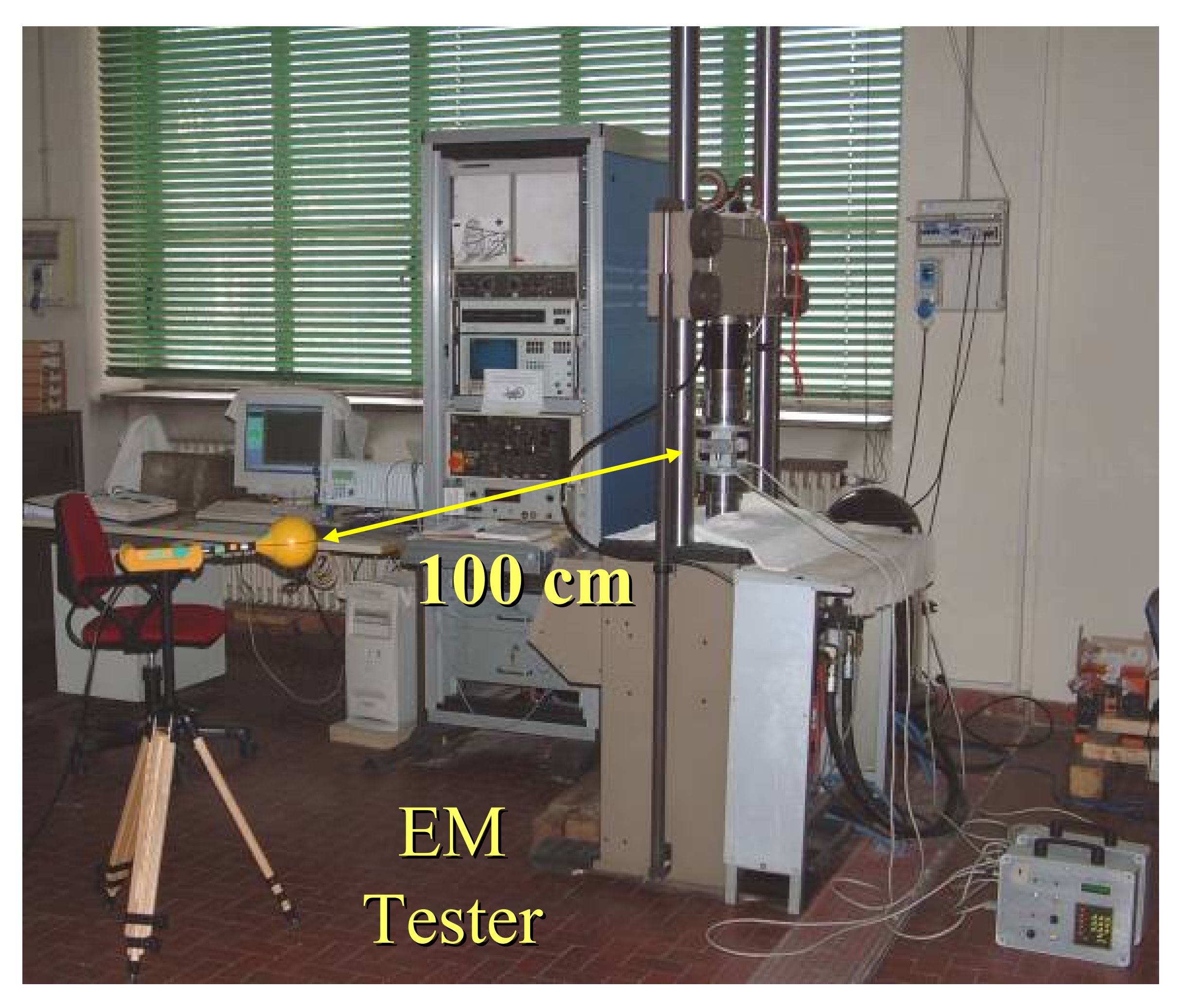

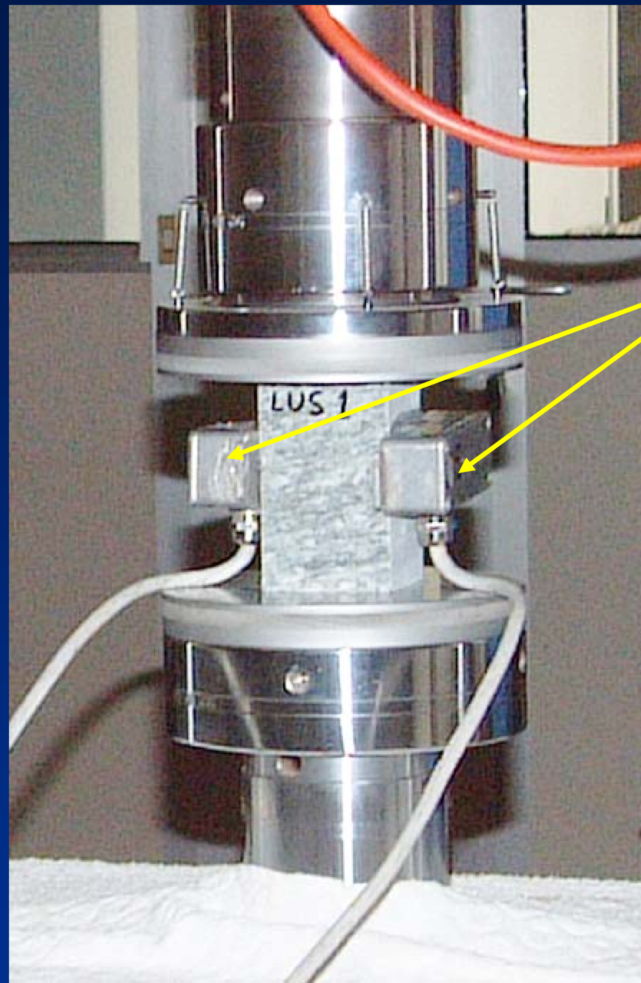

The outputs of the AE transducer and the EM tester were connected to an oscilloscope in order to acquire simultaneously AE and EME signals associated with the same fracture event (10 M Samples s^{-1}).

A model for EME origin

Frid et al. (III) and Rabinovitch et al. (IV) recently proposed a general mechanism to explain the EME origin, which does not require any specific properties (such as piezoelectricity) to take place.

In this model mechanical and electrical equilibrium are broken at the fracture surfaces with creation of ions moving collectively.

Lines of positive ions on both newly created faces oscillate collectively around their equilibrium positions in opposite phase to the negative ones.

The resulting oscillating dipoles created on both faces of the propagating fracture act as the source of EME.

(III) Frid ,V., Rabinovitch, A. and Bahat, D. "Fracture induced electromagnetic radiation", *J. Phys. D.*, 36, 1620-1628 (2003).

(IV) Rabinovitch, A., Frid, V. and Bahat, D. "Surface oscillations. A possible source of fracture induced electromagnetic oscillations", *Tectonophysics*, 431, 15-21 (2007).

“Snap-back” instability

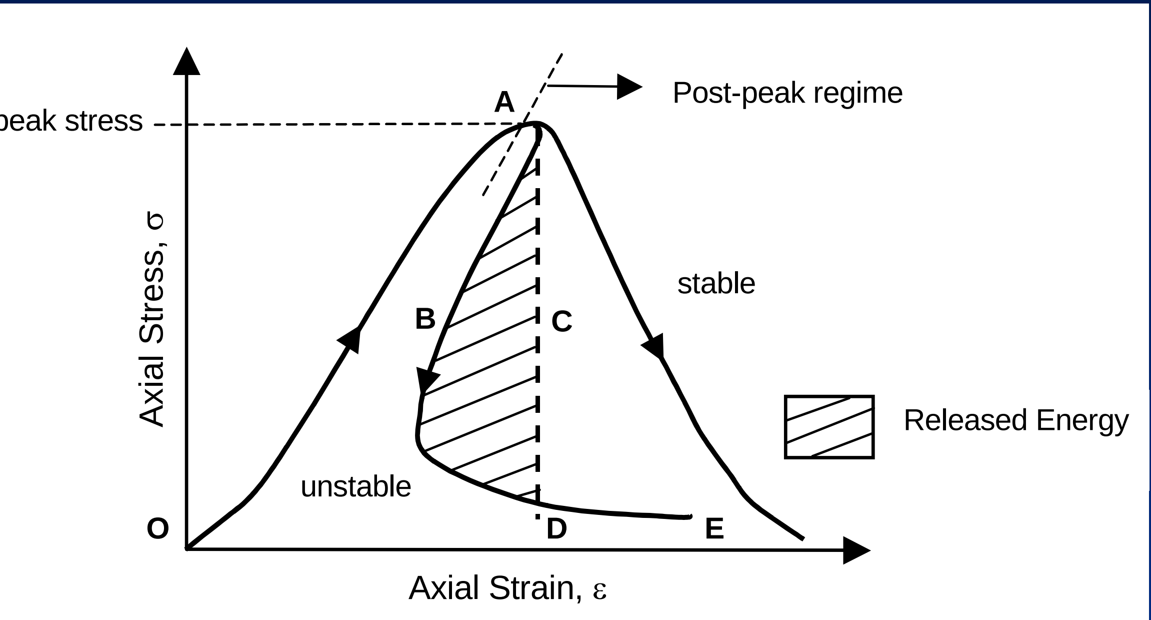

Propagating fracture as EME source

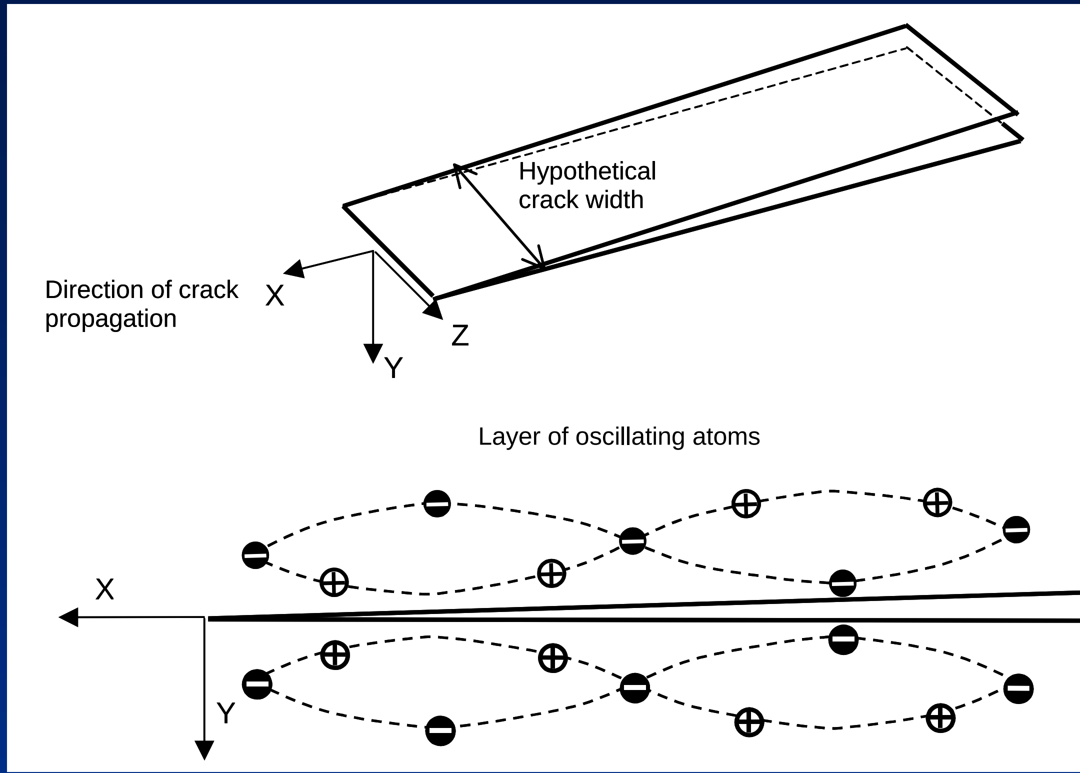

This model correctly accounts for the occurrence of EME associated with abrupt stress drops(V) in load–time diagrams which accompany discontinuous crack propagation.

(V) Carpinteri, A., “Cusp catastrophe interpretation of fracture instability”, *J. of Mechanics and Physics of Solids*, 37 (5), 567-582 (1989).

Experimental set-up

Views of the test specimens

(a)

Concrete

(b)

Luserna Granite

(c)

Carrara Marble

(d)

Syracuse Limestone

Materials, shapes, sizes of the tested specimens and piston velocities

SPECIMEN	MATERIAL	SHAPE	VOLUME [cm^3]	PISTON VELOCITY [$m\ s^{-1}$]
P1	Concrete	Cubic	$10\times10\times10$	0.5×10^{-6}
P2	Carrara Marble	Prismatic	$6\times6\times10$	0.5×10^{-6}
P3	Green Luserna Granite	Prismatic	$6\times6\times10$	2.0×10^{-6}
P4	Syracuse Limestone	Cylindrical	$\pi\times2.5^2\times10$	1.0×10^{-6}

Concrete Specimen P1 - Load vs. Time Curve

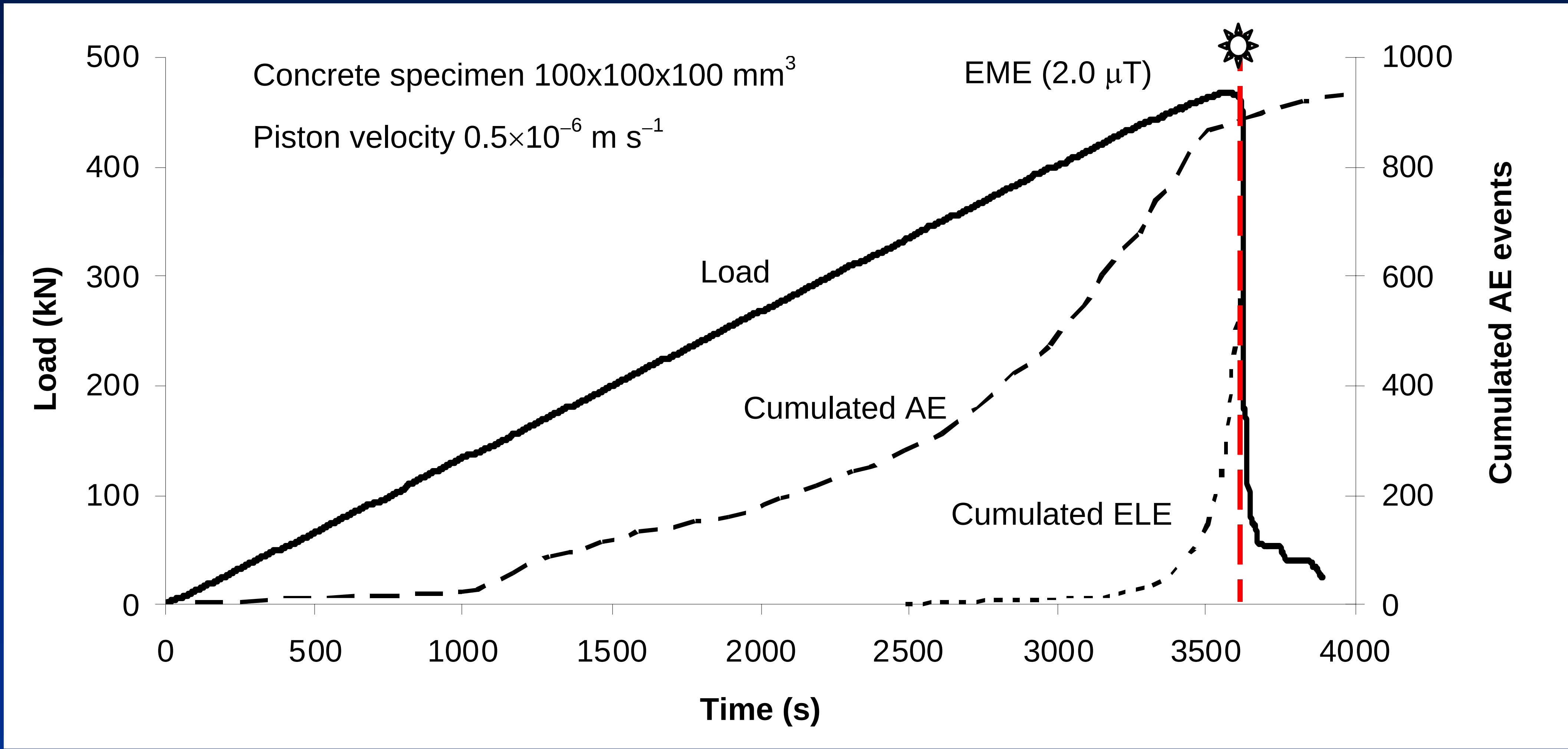

The dashed line represent the cumulated number of AE (high-frequency) while the dotted line the ELE (low-frequency).

The star on the graph shows the moment of EME event with magnetic component of 2.0 μT.

Carrara Marble Specimen P2 - Load vs. Time Curve

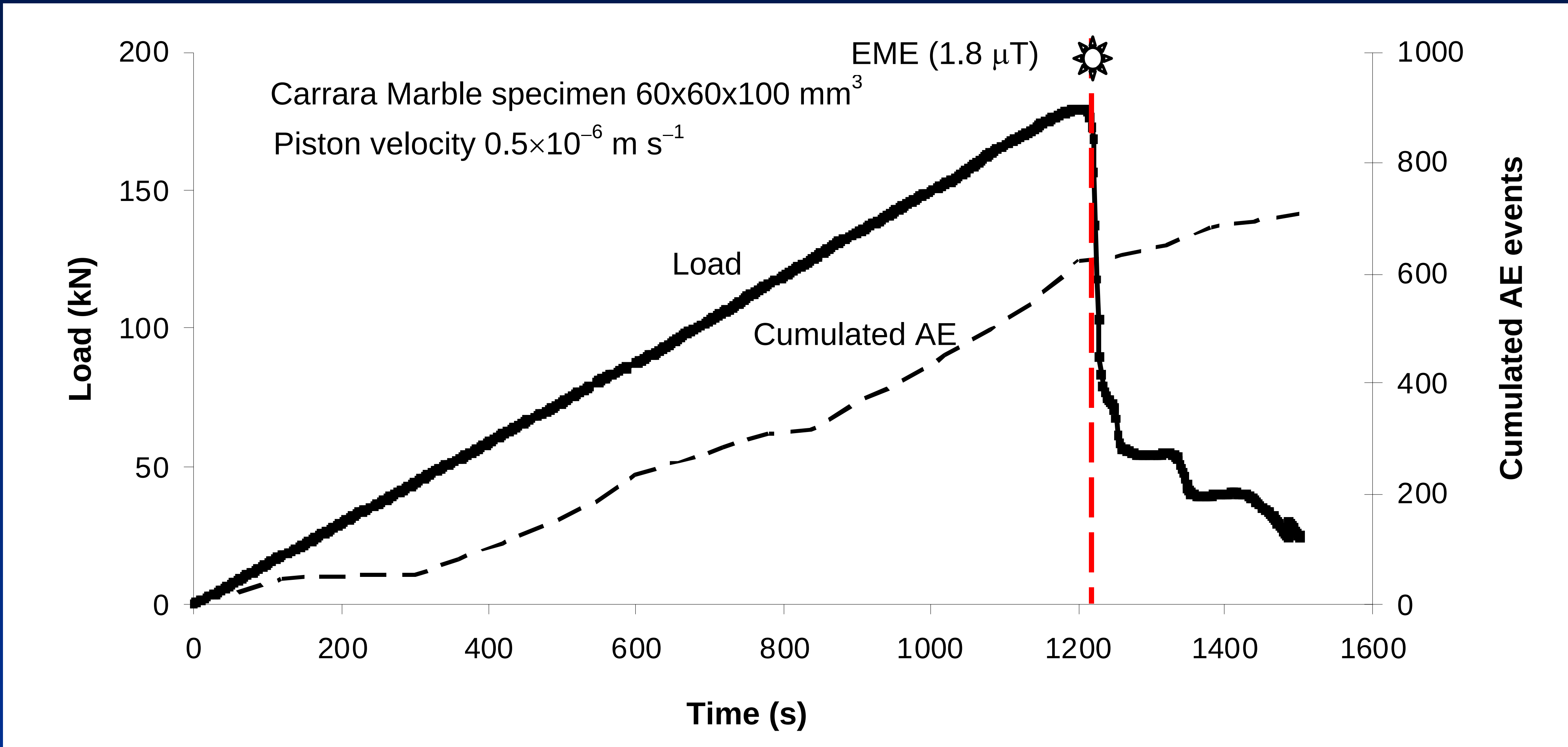

The dashed line represents the cumulated number of AE-HF.

The star on the graph shows the moment of EME event with magnetic component of 1.8 μT.

Luserna Granite Specimen P3 - Load vs. Time Curve

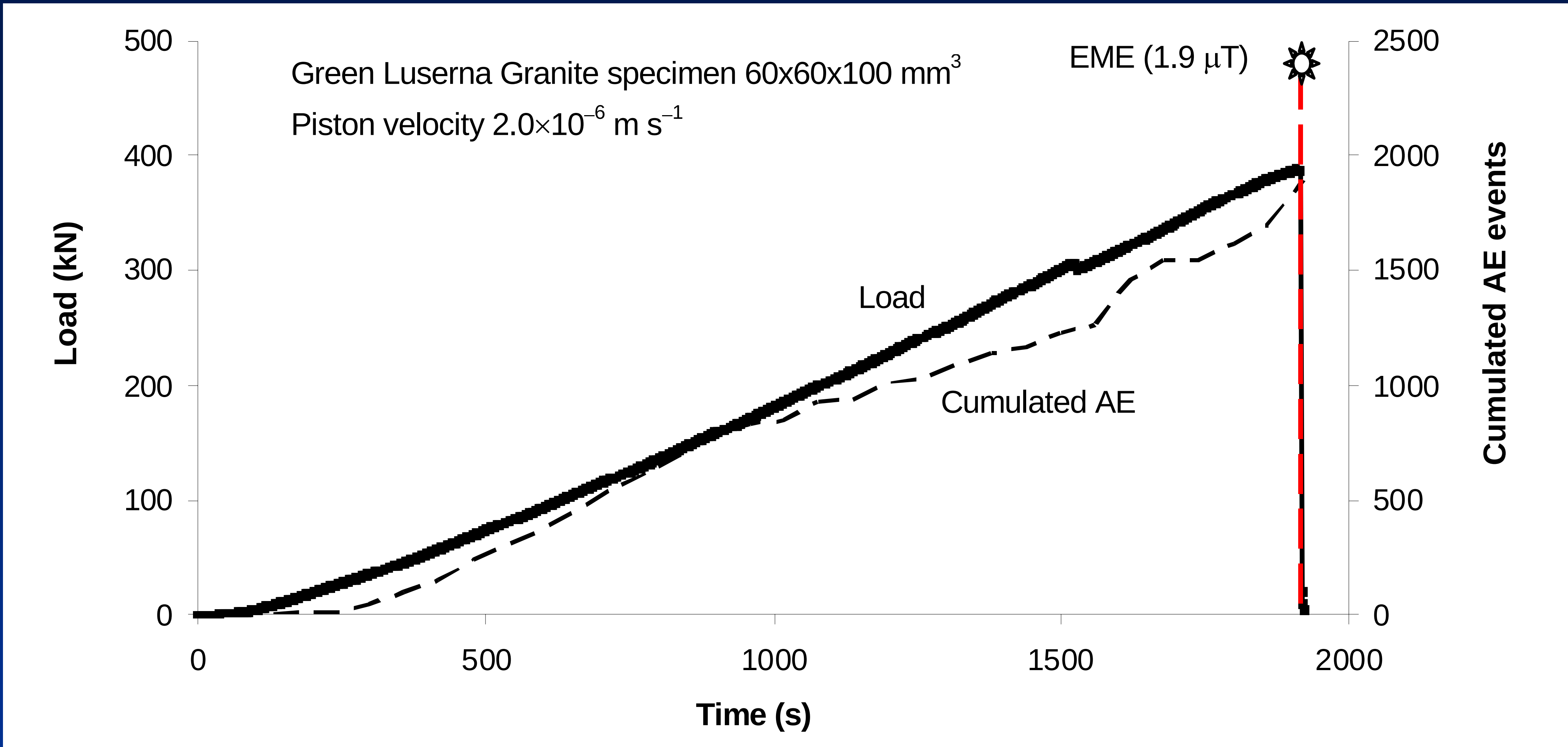

The dashed line represents the cumulated number of AE-HF.

The star on the graph shows the moment of EME event with magnetic component of 1.9 μT.

Syracuse Limestone Specimen P4 - Load vs. Time Curve

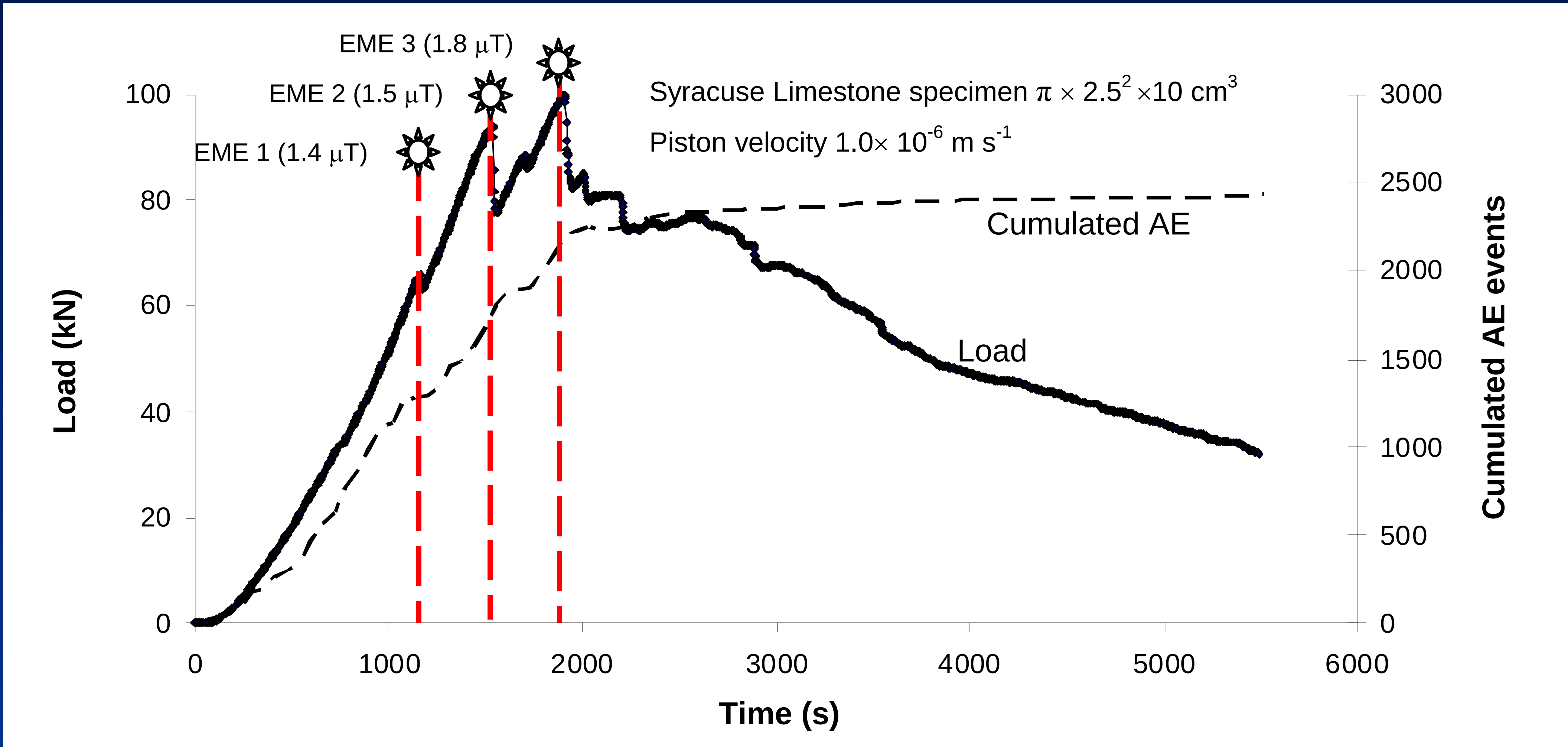

The dashed line represents the cumulated number of AE-HF.

The stars on the graph show the moments of EME events with magnetic component comprised between 1.4 and 1.8 μT.

Syracuse Limestone Specimen P4 - Load vs. Time Curve

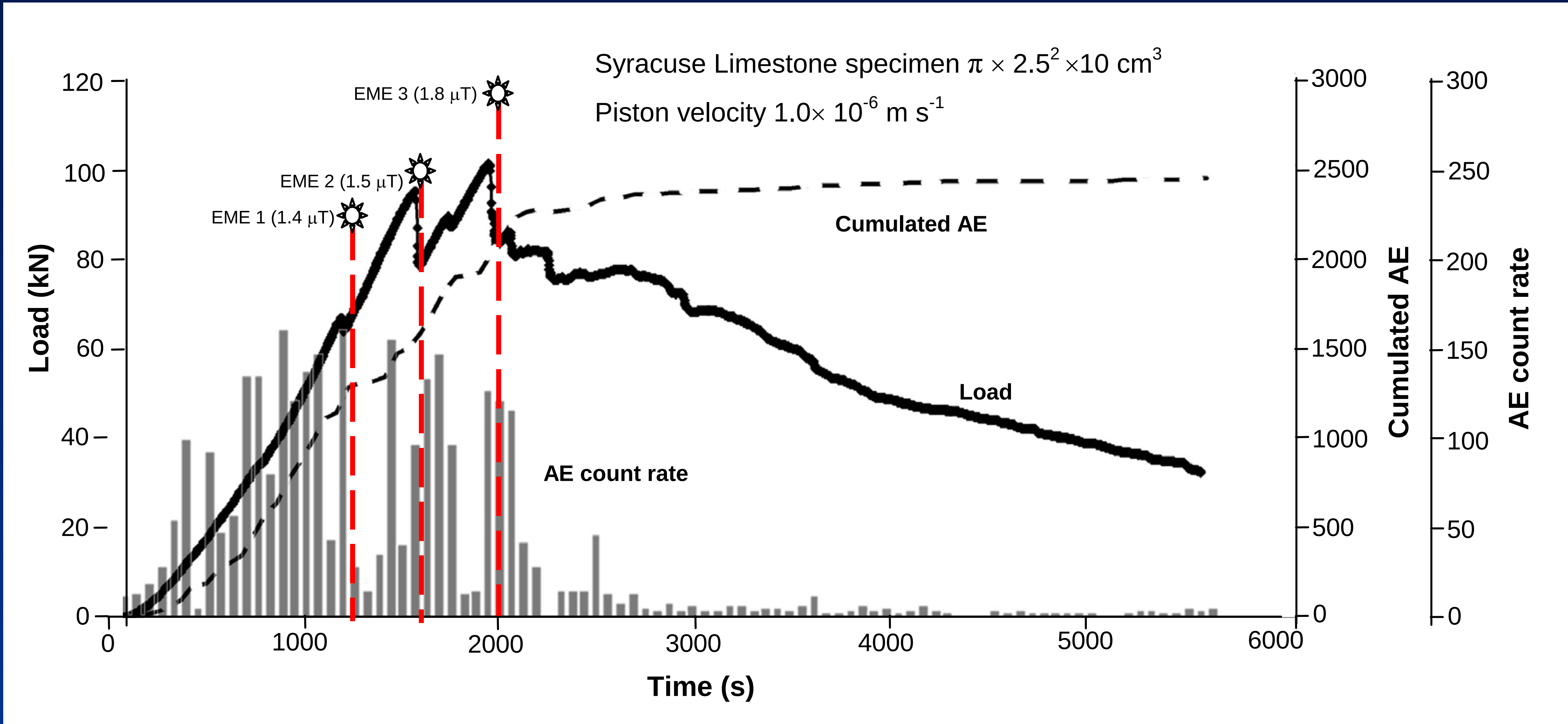

The dashed line represents the cumulated number of AE-HF, the histograms represent the AE-HF count rate.

After the stress drops, acoustic emissions are very low during the reloading of the material until the stress exceeds the previous reached values.

Syracuse Limestone Specimen P4

Displacement rate: **1.0×10^{-6} s^{-1}**

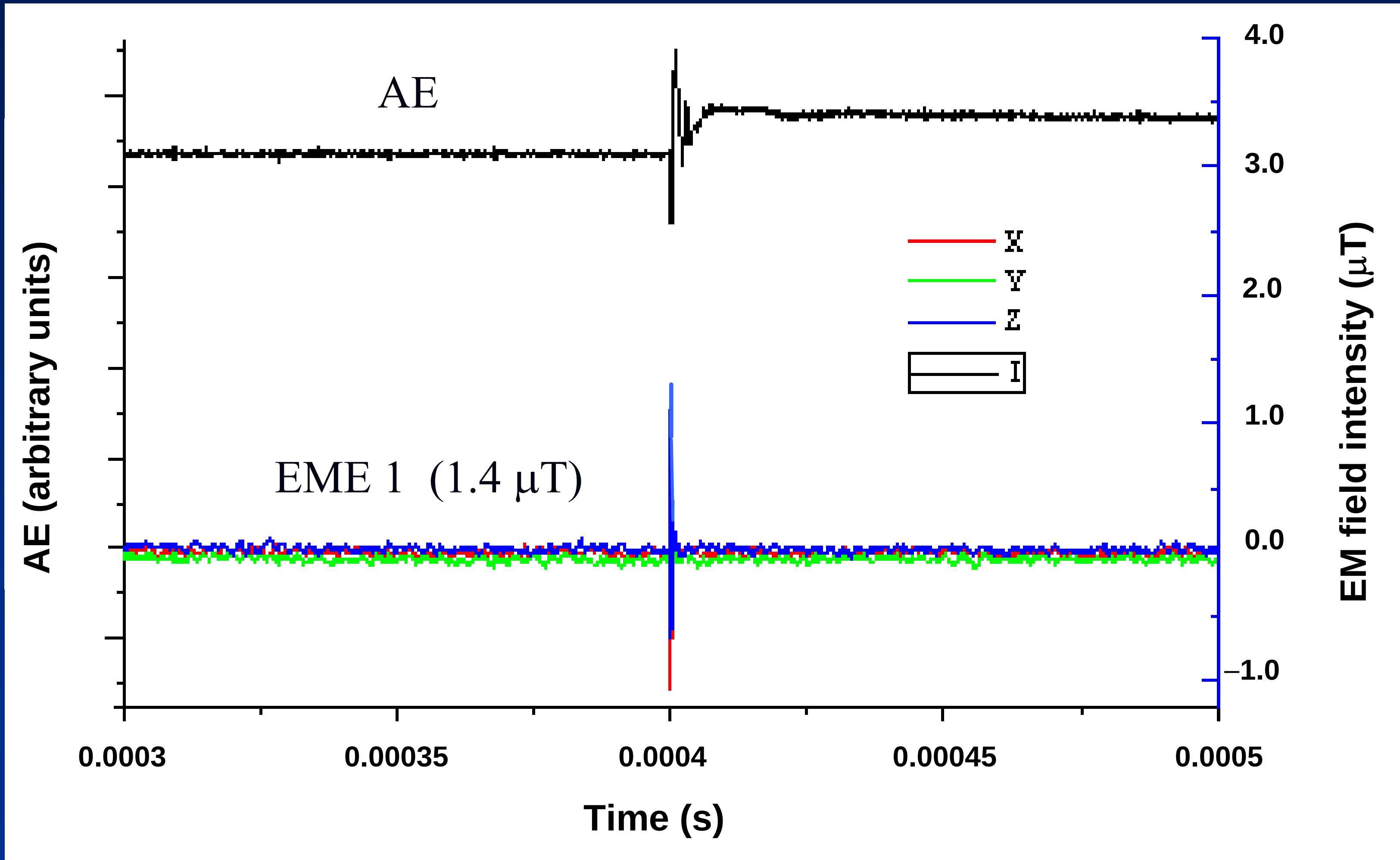

A pair of AE and EME signals associated with the same fracture event.

Detailed AE data analysis on the Concrete Specimen P1

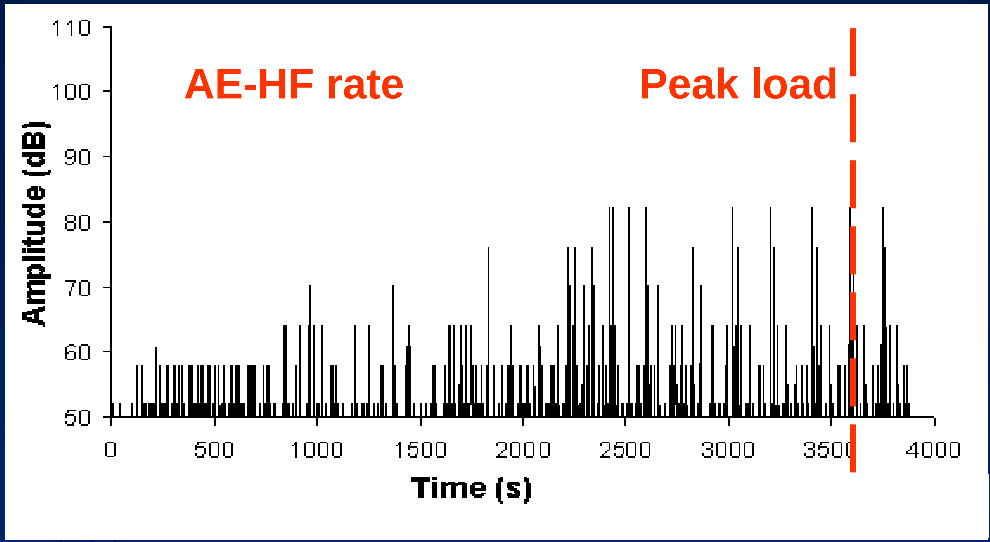

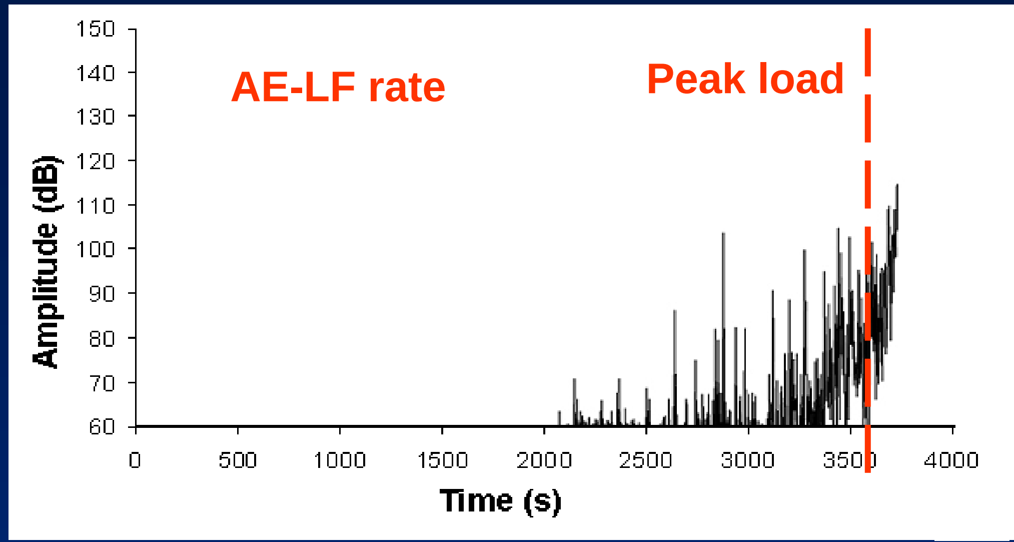

AE-HF and AE-LF time history on Concrete Specimen P1.

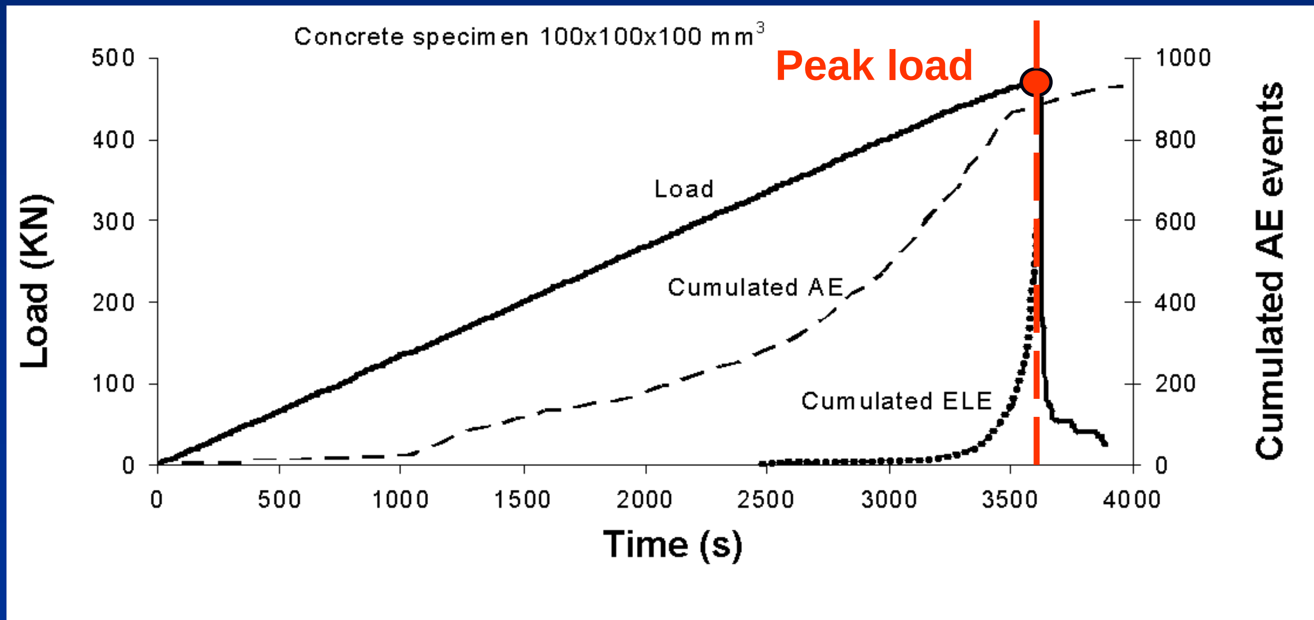

Load vs. time diagram represented with cumulative AE-HF and AE-LF counts for each minute of the testing time.

AE low-frequency signals spectral contents

Before the peak load

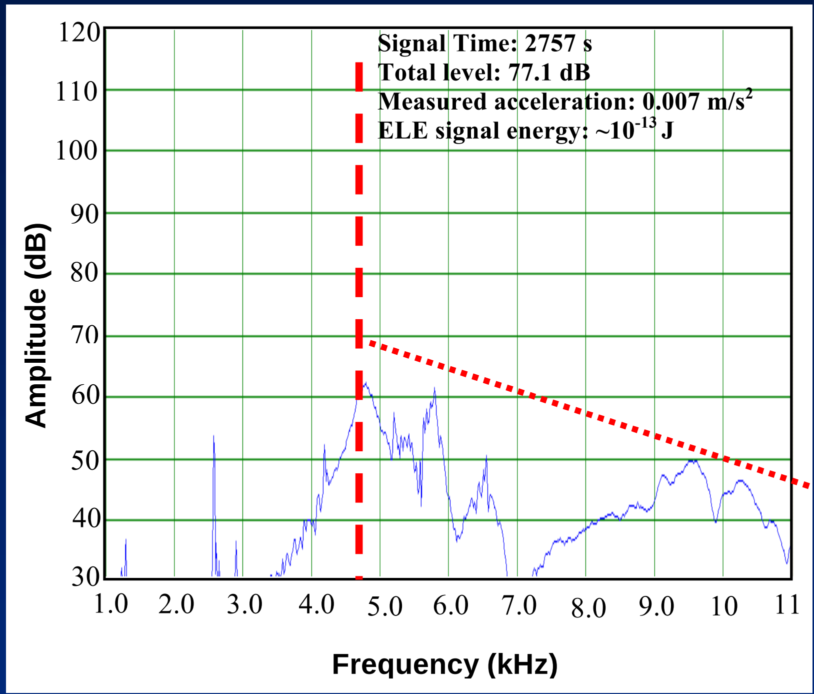

After the peak load

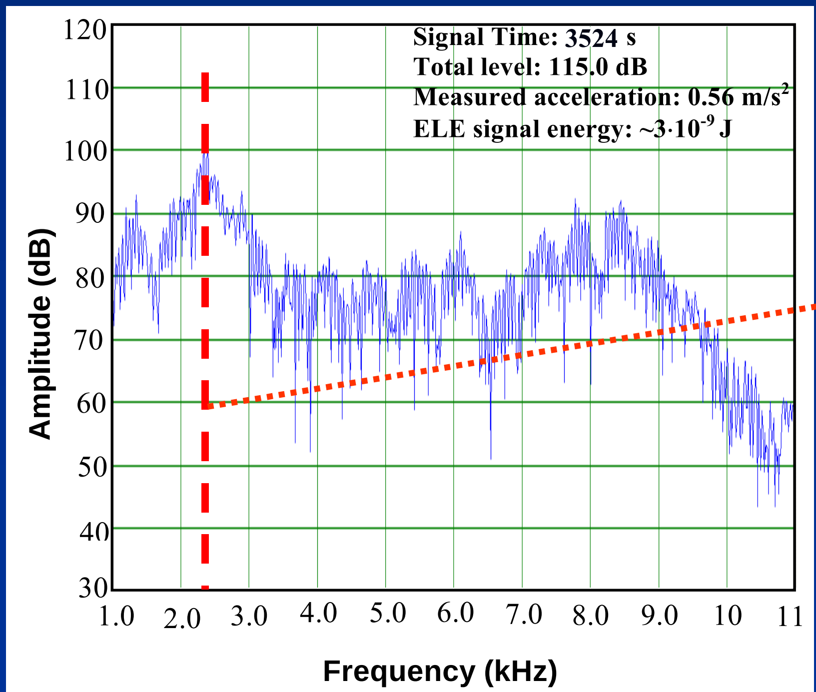

Peak frequencies time history

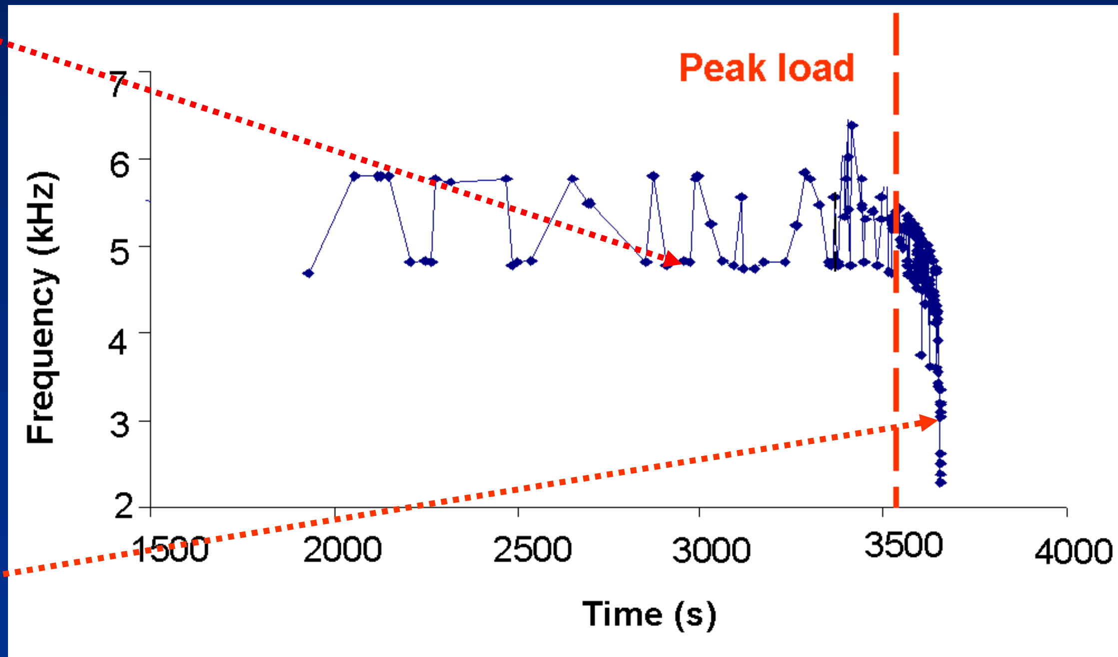

AE Frequency-Magnitude Statistics

The GR relationship has been tested successfully in the acoustic emission field to study the scaling of the ‘‘amplitude distribution’’ in AE waves:

$$Log_{10}N(\geq m) = a - bm, \quad \text{or} \quad N(\geq m) = 10^{a-bm}, \qquad (1)$$

***N* : cumulative number of AE events with magnitude ≥ *m*.**

The *magnitude* in terms of AE technique is defined as follows:

$$m = Log_{10}A_{\max} + f(r), \qquad (2)$$

A_{max} : signal amplitude, measured in microvolt;

***f*(*r*) : correction taking into account that the amplitude is a decreasing function of the distance *r* between the source and the sensor.**

The *b*-value changes systematically with the different stages of fracture growth and hence it can be used to estimate the development of fracture process.

In particular, recent results(VI)(VII) from AE laboratory tests on different types of specimens, as well as *in situ* AE investigations, show that at the condition of criticality, when the external load equals the peak load:

$$b\text{-value} \cong 1.5.$$

In the later stages of damage evolution, when the final failure is imminent:

$$b\text{-value} \rightarrow 1.$$

(VI) Carpinteri, A., Lacidogna, G., Puzzi, S., "From criticality to final collapse: evolution of the "*b*-value" from 1.5 to 1.0", *Chaos, Solitons & Fractals*, 41, 843-853 (2009).

(VII) Carpinteri, A., Lacidogna, G., Niccolini, G., Puzzi, S., "Critical defect size distributions in concrete structures detected by the acoustic emission technique", *Meccanica*, 43, 349-363 (2008).

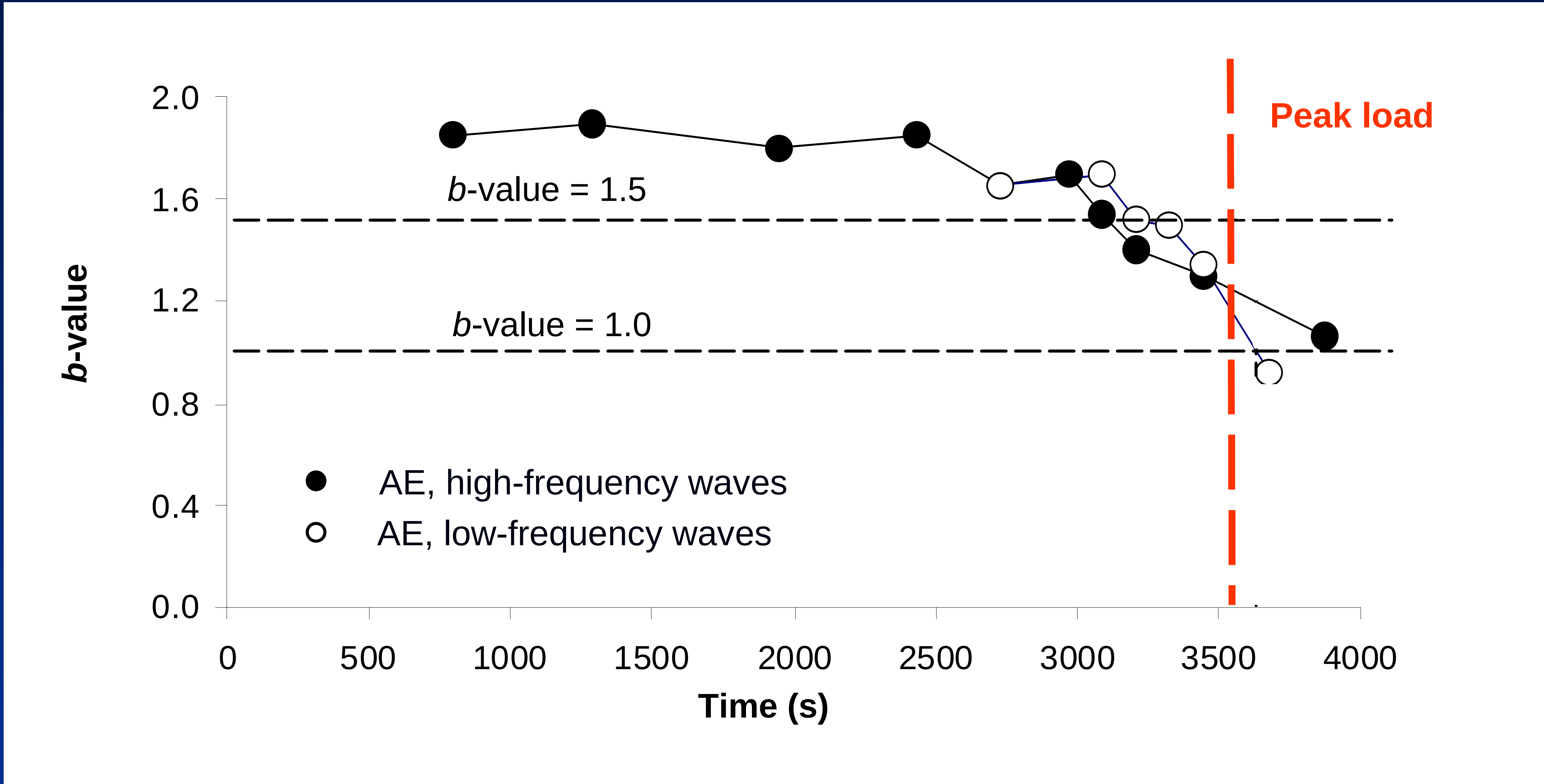

Trends of the *b*-value computed for AE and ELE signals.

Relation between EME and stress drops

Cylindrical Luserna Granite specimen, Volume: $\pi \times 1.4^2 \times 2.8$ cm^3

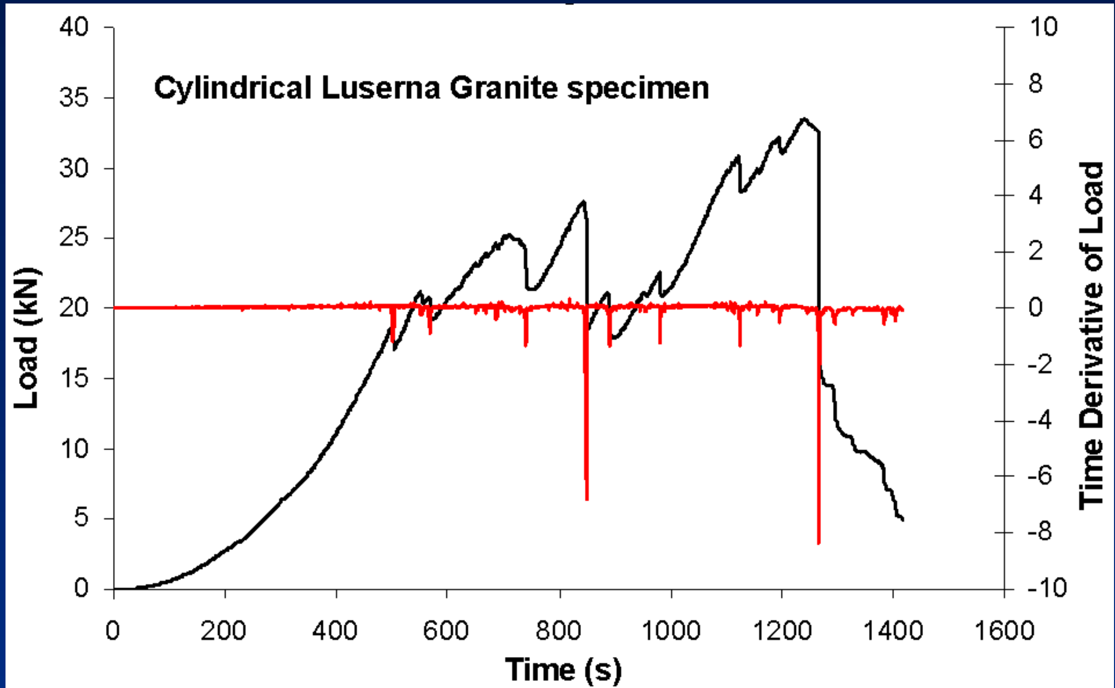

Load vs. time curve and time derivative of load up to the final failure.

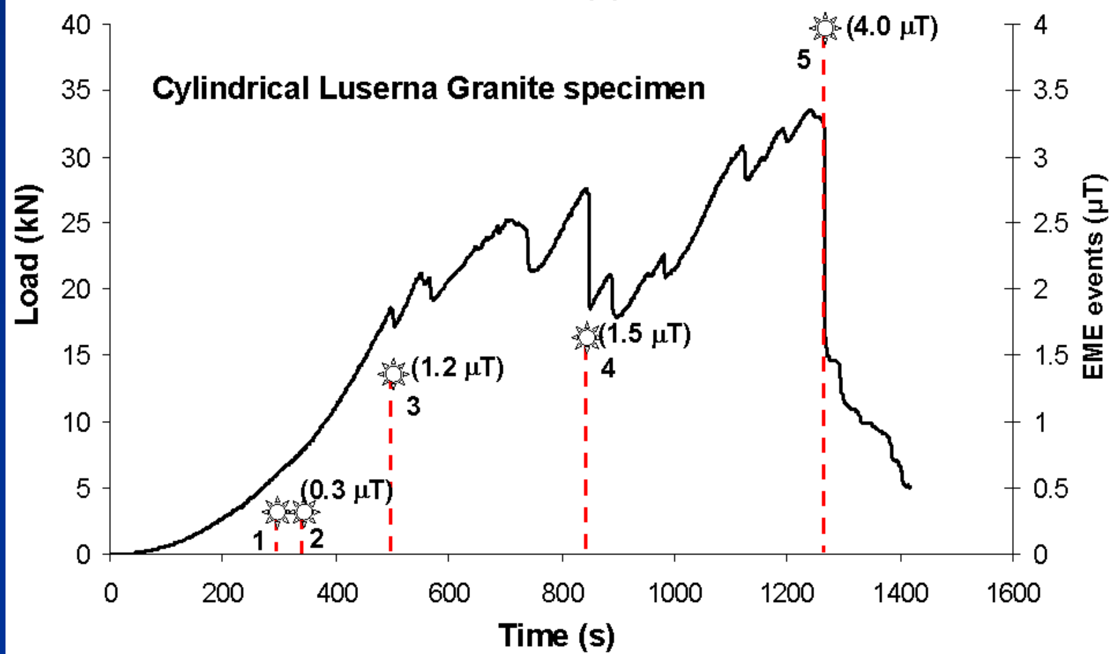

Load vs. time curve and EME events with their magnetic component.

Relation between EME and compression stress

Recently proposed relations(VIII) (IX) between stress and EME events generally show that increasing the stress level, the EME intensity grows.

From our experiments the relation can be well approximated by: $E \propto \Delta\sigma^2$

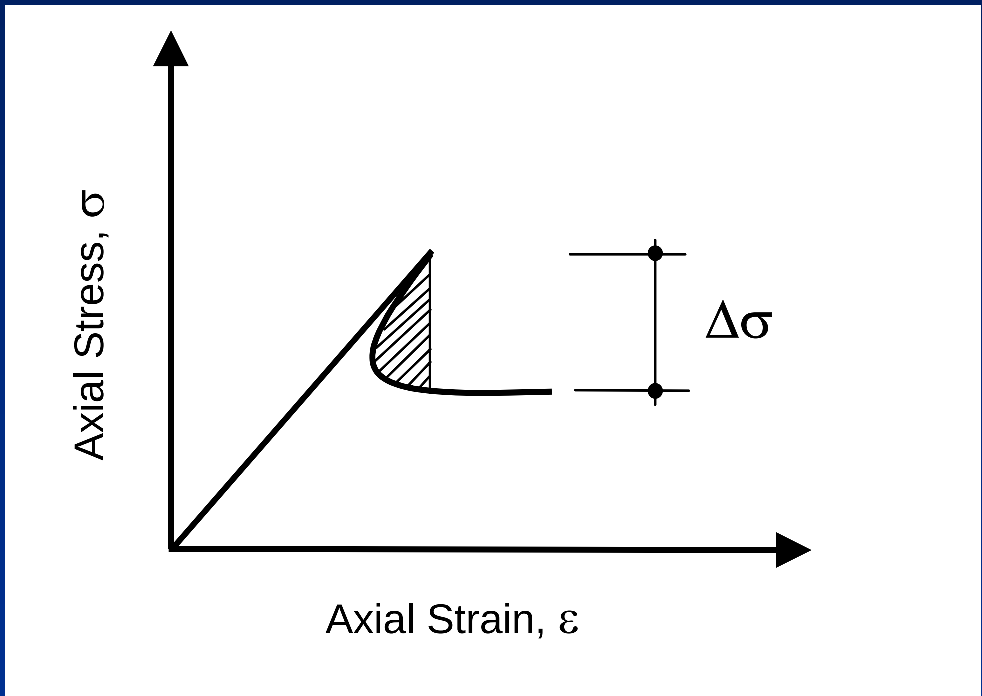

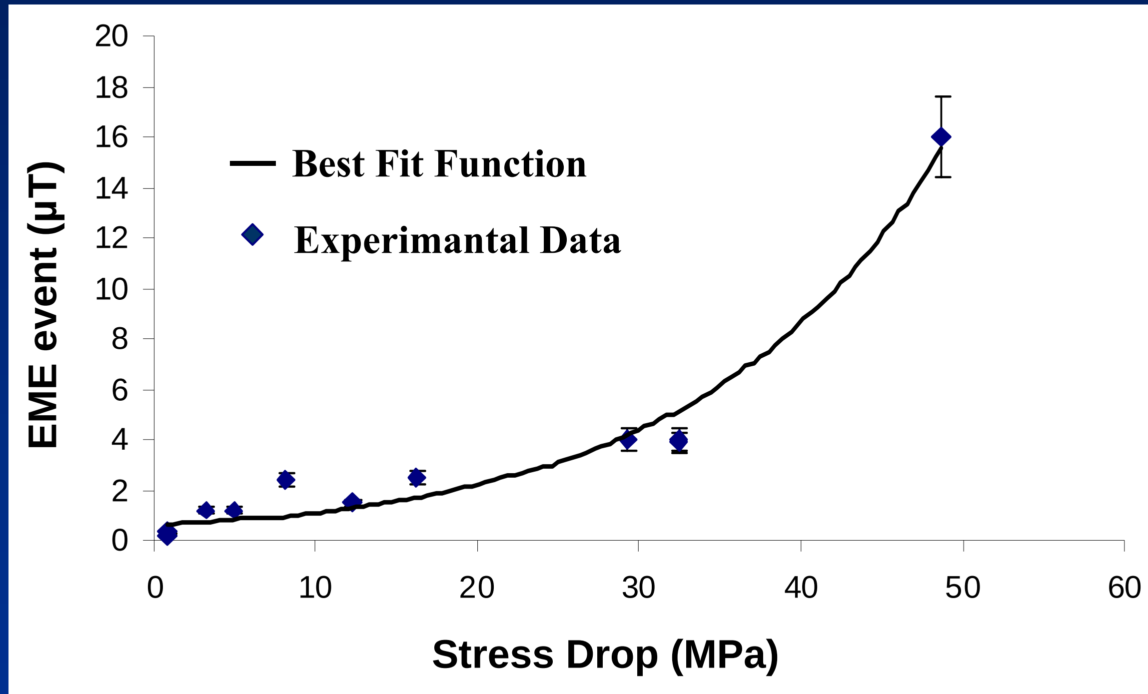

VIII) Wan, G. , Li, X. and Hong, L. "Piezoelectric responses of brittle rock mass containing quartz to static stress and exploding stress wave respectively", *J. Cent. South Univ. Technol.*, 15, 344-349 (2008).

IX) Fukui, K., Okubo ,S., and Terashima T. "Electromagnetic radiation from rock during uniaxial compression testing", *Rock Mech. Rock Engng.*, 38, 411-423 (2005).

Conclusions

- The experimental observations confirm the occurrence of AE and EME signals as failure precursors in materials like rocks and concrete.
- The simultaneous detection of AE and EME signals is an evidence that cracking generates temporally varying EM fields.
- In all tested materials the EME events are associated to abrupt stress drops suggesting that EME originates from crack propagation.
- Mechanisms such as electrification due to friction effects seem to be excluded by the experimental observations.
- In fact, we don’t detect EME during post-failure stages, manly characterized by friction due to sliding of the existing crack faces.
- As AE and EME have been observed before the onset of earthquakes, detection of these phenomena during laboratory experiments looks promising for effective applications at structural and geological scales.